

CMR Imaging of Edema in Myocardial Infarction Using Cine Balanced Steady-State Free Precession

Andreas Kumar, MD, MSc,* Nirat Beohar, MD,‡ Jain Mangalathu Arumana, DIPL ING,§
Eric Larose, MD,* Debiao Li, PhD,§|| Matthias G. Friedrich, MD,†
Rohan Dharmakumar, PhD§||

Québec City, Québec, Calgary, Alberta, Canada; Chicago, Illinois; and Los Angeles, California

OBJECTIVES The aim of this study was to investigate the capabilities of balanced steady-state free precession (bSSFP) cardiac magnetic resonance imaging as a novel cine imaging approach for characterizing myocardial edema in animals and patients after reperfused myocardial infarction.

BACKGROUND Current cardiac magnetic resonance methods require 2 separate scans for assessment of myocardial edema and cardiac function.

METHODS Mini-pigs (n = 13) with experimentally induced reperfused myocardial infarction and patients with reperfused ST-segment elevation myocardial infarction (n = 26) underwent cardiac magnetic resonance scans on days 2 to 4 post-reperfusion. Cine bSSFP, T2-weighted short TI inversion recovery (T2-STIR), and late gadolinium enhancement were performed at 1.5-T. Cine bSSFP and T2-STIR images were acquired with a body coil to mitigate surface coil bias. Signal, contrast, and the area of edema were compared. Additional patients (n = 10) were analyzed for the effect of microvascular obstruction on bSSFP. A receiver-operator characteristic analysis was performed to assess the accuracy of edema detection.

RESULTS An area of hyperintense bSSFP signal consistent with edema was observed in the infarction zone (contrast-to-noise ratio: 37 ± 13) in all animals and correlated well with the area of late gadolinium enhancement ($R = 0.83$, $p < 0.01$). In all patients, T2-STIR and bSSFP images showed regional hyperintensity in the infarction zone. Normalized contrast-to-noise ratios were not different between T2-STIR and bSSFP. On a slice basis, the volumes of hyperintensity on T2-STIR and bSSFP images correlated well ($R = 0.86$, $p < 0.001$), and their means were not different. When compared with T2-STIR, bSSFP was positive for edema in 25 of 26 patients (96% sensitivity) and was negative in all controls (100% specificity). All patients with microvascular obstruction showed a significant reduction of signal in the subendocardial infarction zone compared with infarcted epicardial tissue without microvascular obstruction ($p < 0.05$).

CONCLUSIONS Myocardial edema from ST-segment elevation myocardial infarction can be detected using cine bSSFP imaging with image contrast similar to T2-STIR. This new imaging approach allows evaluation of cardiac function and edema simultaneously, thereby reducing patient scan time and increasing efficiency. Further work is necessary to optimize edema contrast in bSSFP images. (J Am Coll Cardiol Img 2011;4:1265–73) © 2011 by the American College of Cardiology Foundation

From the *Heart and Lung Institute, Laval University, Québec City, Québec, Canada; †Stephenson Cardiovascular Magnetic Resonance Centre at the Libin Cardiovascular Institute of Alberta, University of Calgary, Calgary, Alberta, Canada; ‡Department of Cardiology, Northwestern University, Chicago, Illinois; §Department of Radiology, Northwestern University, Chicago, Illinois; and the ||Biomedical Imaging Research Institute, Department of Biomedical Sciences, Cedars-Sinai Medical Center, Los Angeles, California. This work was supported by grants from NIH/NHLBI (HL091989) and the American Heart Association (SDG 0735099N). Dr. Friedrich is currently affiliated with the Montreal Heart Institute, Department of Cardiology, Université de Montréal, Montréal, Québec, Canada. During this study, Dr. Kumar was a Canadian Institutes of Health Research (CIHR) strategic training fellow in TORCH (Tomorrow's Research in Cardiovascular Health Professionals). Dr. Kumar holds a research grant from the Canadian Institutes of Health Research; receives financial support for

T2-weighted cardiac magnetic resonance (CMR) has been successfully used for differentiating acute from chronic myocardial infarction (MI) based on elevations in myocardial T2 due to tissue edema accompanying acute, but not chronic, MI (1). Furthermore, T2-weighted assessment of myocardial edema may allow the detection of acute coronary syndromes (2,3) as well as the assessment of the area at risk and myocardial salvage (4).

Currently, T2-weighted CMR is performed using fast spin-echo sequences, with double or triple inversion preparation to suppress signal from intracavity blood and/or fat (1) or with a T2 preparation with balanced steady-state free precession (bSSFP) readouts (5). Covering the entire left ventricle with T2-weighted CMR takes 8 to 15 min, which is undesirable in the setting of a possible acute coronary syndrome or acute myocardial infarction (AMI). Because these acquisitions are limited to a single cardiac phase, additional multiphase (cine) scans are required to evaluate cardiac function, which significantly extends the duration of the clinical examinations.

An alternate approach to ascertaining the presence of myocardial edema may be available through bSSFP imaging. Cine bSSFP imaging is a clinically established CMR method for the assessment of left and right ventricular volumes and function. It is known that bSSFP signals are influenced by T1, T2 (6), and magnetization transfer effects (7). With increased free water resulting from edema, T1 and T2 are both increased (8), and magnetization transfer is reduced (9). Although T2 and T1 effects are antagonistic in the setting of bSSFP imaging and will work to reduce the overall effect of relaxation

changes, with the residual relaxational contribution combined with alterations in magnetization transfer (10), it may be possible to visualize reperfused acute myocardial infarct territories as hyperintense zones relative to healthy/remote myocardium. Using bSSFP imaging to detect edema in the setting of

reperfused AMI would have important implications: 1) increased efficiency of cardiac examinations; and 2) coregistration of cardiac function and tissue characterization for clinical use.

The aim of this study was to investigate whether bSSFP imaging can be used to visualize the presence of edema in AMI in a controlled swine model as well as in patients with acute reperfused ST-segment elevation myocardial infarction (STEMI), using a control group of healthy volunteers. We hypothesized that: 1) in animals and patients with reperfused AMI, bSSFP will yield a hyperintense signal in the infarction zone compared with the remote zone; and 2) in healthy volunteers, bSSFP signals are homogeneous throughout the myocardium in the absence of edema, as determined by T2-STIR imaging.

METHODS

Animal studies. The animal study protocol was reviewed and approved by the Institutional Animal Care and Use Committee.

ANIMAL PREPARATION. In 15 Yucatan mini-pigs (body weight 25 to 30 kg), MI was induced as follows. The animals were anesthetized and mechanically ventilated with isoflurane. The right femoral artery was cannulated, and a guide catheter was advanced into the left circumflex artery. A balloon catheter was positioned in the proximal third of the artery and inflated to achieve complete occlusion of the artery. Success of coronary artery occlusion was controlled angiographically and by electrocardiographic recording of ST segment elevation. The occlusion was released after 90 min, and animals were allowed to recover for 2 to 3 days.

Before CMR imaging, each mini-pig was sedated, intubated, and placed on a ventilator, and systemic O₂ saturation, end-tidal PCO₂, and heart rate were continuously monitored.

IMAGING PROTOCOL. All animal studies were performed on a clinical 1.5-T CMR system (Sonata, Siemens, Erlangen, Germany). Animals were positioned in a feet-first right-anterior oblique position,

ABBREVIATIONS AND ACRONYMS

bSSFP = balanced steady-state free precession

CMR = cardiac magnetic resonance

CNR = contrast-to-noise ratio

LGE = late gadolinium enhancement

MVO = microvascular obstruction

ROI = region of interest

SI = signal intensity

STEMI = ST-segment elevation myocardial infarction

T2-STIR = T2-weighted short T1 inversion recovery

TE = echo time

TI = inversion time

TR = repetition time

investigator-initiated research from Pfizer Canada; and is a medical advisor to Nordic Biotech. Drs. Li and Dharmakumar hold research grants from the National Institutes of Health/National Heart, Lung, and Blood Institute; and both receive research support from Siemens Healthcare. Dr. Dharmakumar also holds a research grant from the American Heart Association. Dr. Friedrich holds research grants from the Canadian Institutes of Health Research, the Canadian Diabetes Association, the Alberta Heritage Foundation for Medical Research, and the Heart and Stroke Foundation of Canada; receives research support from Husky Energy, Pfizer Canada, and Siemens Canada; and is a shareholder in and scientific advisor to Circle Cardiovascular Imaging. All other authors have reported that they have no relationships relevant to the contents of this paper to disclose.

Manuscript received August 10, 2010; revised manuscript received March 9, 2011, accepted April 7, 2011.

and a flexible, phased-array surface coil was placed over the chest. Scout images were obtained to localize the true axes of the heart, and whole-heart shimming was performed. Subsequently, multiple contiguous short-axis 2-dimensional bSSFP images were acquired in the cine mode covering the whole left ventricle using a standard cine bSSFP sequence (scan parameters: voxel size = $0.9 \times 0.9 \times 6$ mm³; flip angle = 65°; repetition time [TR]/echo time [TE] = 3.1/1.5 ms; readout bandwidth = 930 Hz/pixel; 25 cardiac phases) with 2 to 3 signal averages. Subsequently, a gadolinium-based contrast agent was injected intravenously (gadolinium-diethylenetriamine pentaacetic acid, Magnevist, Berlex Laboratories Inc., Montville, New Jersey) at a dose of 0.1 mmol/kg, and late gadolinium enhancement (LGE) imaging was performed 10 to 15 min after contrast injection. LGE acquisitions were breath held, triggered to end-systole, and covered the entire left ventricle with the same slice positions used for cine bSSFP imaging. LGE images were acquired in end-systole to have the largest myocardial surface for analysis while minimizing cardiac motion. LGE-CMR images were acquired using an inversion-recovery turbo FLASH sequence with the following scan parameters: TR of 1 R-R interval; TE = 1.1; inversion time [TI] = 200 to 240 ms; flip angle = 25°; voxel size = $1.3 \times 1.3 \times 6$ mm³; and same field of view as bSSFP scans.

Human studies. The study protocol for volunteers and patients was reviewed and approved by the Institutional Ethics Committee, and written informed consent was obtained from each participant.

IMAGING PROTOCOL. All studies in humans were performed on a clinical 1.5-T CMR system (Avanto, Siemens). The anatomic axes of the heart were determined, and a whole-heart shim was performed. In healthy volunteers ($n = 8$, age 30 ± 8 years, 4 women, no evidence of heart disease), a short-axis slice was obtained at a midventricular level using a cine bSSFP sequence followed by a T2-STIR sequence. In patients (27 patients without microvascular obstruction [MVO] as defined by LGE, and 10 patients with MVO, all enrolled within 4 days after successful angioplasty for a first STEMI, as defined by American Heart Association diagnostic criteria), the sequences were prescribed along the midventricular short-axis slice. LGE-CMR was performed with the same gadolinium diethylenetriamine pentaacetic acid dose and imaging sequence. Typical imaging parameters for bSSFP were field of view of 340×276 mm, imaging matrix of 192×156 , slice thickness of 10

mm, flip angle of 65°, TR/TE of 3.32/1.16 ms, bandwidth of 930 Hz/pixel, and 25 cardiac phases. Typical imaging parameters for T2-STIR imaging were field of view of 380×309 mm, matrix of 256×208 , slice thickness of 10 mm, mid-diastolic acquisition, echo-train length of 25, TR of 2 heart beats, TE of 61 ms, and bandwidth of 245 Hz/pixel. Both bSSFP and T2-STIR images were acquired with the body coil. Typical LGE-CMR imaging parameters were TR of 1 R-R interval, TE of 3.32 ms, bandwidth of 235 Hz/pixel, field of view of 400×300 mm, imaging matrix of 256×192 , and slice thickness of 10 mm. No image-acceleration methods were used in this study.

Image analysis. ANIMALS. CMR analysis was performed to test for infarction-dependent signal differences on bSSFP as follows: based on slice position and trigger time, LGE-CMR and cine bSSFP images were matched. Image analysis was performed using Matlab 7.0 (MathWorks, Natick, Massachusetts). On the basis of LGE-CMR images, remote (noninfarcted) regions of the myocardium were identified, and the mean (signal intensity of the remote myocardium [S_r]) and SD of the signal intensities (SIs) of these regions were computed in the LGE and bSSFP images. Similar to previous studies (1,2), pixels with SIs >2 SD of the remote areas of the bSSFP images were identified as regions of edema and were used to compute the mean signal within the hyperintense zones (S) and total area of edema. The infarct zone was identified as the myocardial region with SIs >5 SD of the mean SI from the remote regions, as described previously (11). Using this criterion, the infarct zones were identified on a pixel-by-pixel basis, and the total infarct areas and the corresponding average SIs of the infarct areas were computed. This was performed on every imaging slice positive for LGE-CMR. From the measured bSSFP SIs, average signal-to-noise ratios (SNRs) of infarction zones were computed for each animal, using $SNR = S/\sigma$, where σ was the SD of noise (air). Contrast-to-noise ratios (CNRs) were computed using $CNR = (S - S_r)/\sigma$.

HEALTHY VOLUNTEERS. In healthy volunteers, myocardial signal homogeneity was assessed based on bSSFP and T2-STIR images, using a validated software (cmr⁴², Circle Cardiovascular Imaging Inc., Calgary, Alberta, Canada), to rule out false-positive signal as follows: representative regions of interest (ROIs) were drawn manually on the T2-STIR images in the anterior wall, septum, inferior wall, and lateral wall and copied to the corresponding frame of the cine bSSFP. SIs were measured for

these ROIs. The SNR was computed in a manner similar to that previously described. To assess signal homogeneity throughout the myocardium, the SNRs of ROIs in the anterior, septal, inferior, and lateral walls were compared.

PATIENTS. To assess for myocardial edema, T2-STIR and bSSFP images of patients with acute reperfused MI were analyzed, using cmr⁴² software as follows: based on slice position and trigger times, T2-STIR and cine bSSFP images were matched. On T2-STIR images, an ROI was drawn in remote myocardium not affected by the infarct. Using the threshold-based signal detection, as described previously (animal studies), remote and edematous territories were identified (Fig. 1). The SI of the remote and the area and SI of edematous myocardium were measured. The ROIs were then copied to the bSSFP images, and signal measurements were repeated. In general, contrast was calculated as: $[(\text{mean SI (infarct)} - \text{mean SI (remote)}) / \text{mean SI (remote)}] \times 100\%$. For MVO, contrast was calculated as: $[(\text{mean SI (infarct zone without MVO)} - \text{mean SI (MVO)}) / \text{mean SI (infarct zone without MVO)}] \times 100\%$. MVOs were identified as hypointense regions in LGE images. bSSFP SIs from the MVOs were measured by manually drawing the ROIs in hypointense cores of LGE images and copying them onto the corresponding frame of bSSFP cine images. The contrast-to-noise ratio (CNR) was computed as $[(\text{mean SI (infarct)} - \text{mean SI (remote)}) / \text{SD of noise}]$. To account for the differences in acquisition bandwidth and spatial resolution between T2-STIR and bSSFP images, a normalized CNR (adjusting for voxel volume and imaging BW), defined as $\text{CNR}_{\text{norm}} = \text{SNR}_{\text{norm}}(\text{infarct}) - \text{SNR}_{\text{norm}}(\text{remote})$, was calculated, where

$\text{SNR}_{\text{norm}} = \text{SNR} \times (\text{BW})^{1/2} / \text{voxel volume}$, and BW is bandwidth. Subsequently, threshold-based signal detection was performed on bSSFP and LGE images, as described previously.

Statistics. Signal and contrast values were compared using a paired *t* test for 2 variables, and using 1-way analysis of variance for multiple variables. Pearson's correlation statistics were used to compare signal measurements and areas of pathology. The difference in the threshold-based measurement of area of edema using T2-STIR and bSSFP was measured as an absolute and the percentage difference, and a Bland-Altman plot was created. No correction was made for multiple correlated observations within individuals. Receiver-operator characteristic analysis, taking T2-STIR images to provide the ground truth, was performed using image contrast values computed from regional SI measurements obtained from patients and from healthy volunteers. Image contrast in bSSFP images from volunteers were computed as the relative percentage of signal differences by arbitrarily assigning one of the walls to be edematous and another to be remote. More specifically, contrast values were computed between lateral and septal, anterior and septal, inferior and septal, lateral and anterior, and anterior and inferior walls. In total, 66 contrast values were obtained and used to derive the receiver-operator characteristic curves (26 data points from patients positive for edema, and 40 data points from volunteers not positive for edema). StatPlus:mac Version 5.2.0 (AnalystSoft Inc., Alexandria, Virginia), and SPSS Version 16 for Mac (SPSS Inc., Chicago, Illinois), Microcal Origin 7.0 (OriginLab Corp., Northampton, Massachusetts) were used for data analysis. Values are given as mean \pm SD. Results were deemed significant for $p < 0.05$.

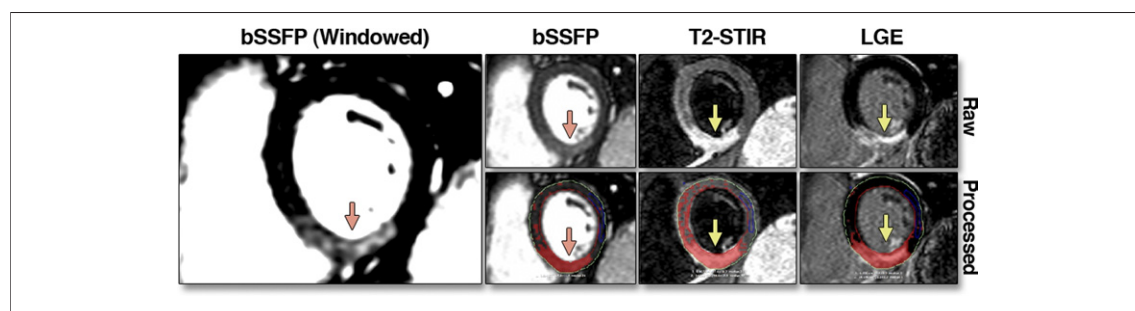


Figure 1. Representative Image Analysis in a 48-Year-Old Man With a First Acute STEMI in the Inferior Territory

The larger image on the left is a windowed balanced steady-state free-precession (bSSFP) image showing hyperintensity in the inferior wall. The right upper panel shows the raw images. The right lower panel shows the same images using semiautomatic threshold-based signal detection. Based on a reference region of interest in remote myocardium (here, the lateral wall), all pixels that have a signal intensity ≥ 2 SD than the mean signal intensity of remote myocardium are automatically highlighted. This example also demonstrates that manual windowing may be necessary to better visualize edematous territories in bSSFP images with the naked eye. Arrows indicate the site of myocardial infarction. LGE = late gadolinium enhancement; STEMI = ST-segment elevation myocardial infarction; T2-STIR = T2-weighted short TI inversion recovery.

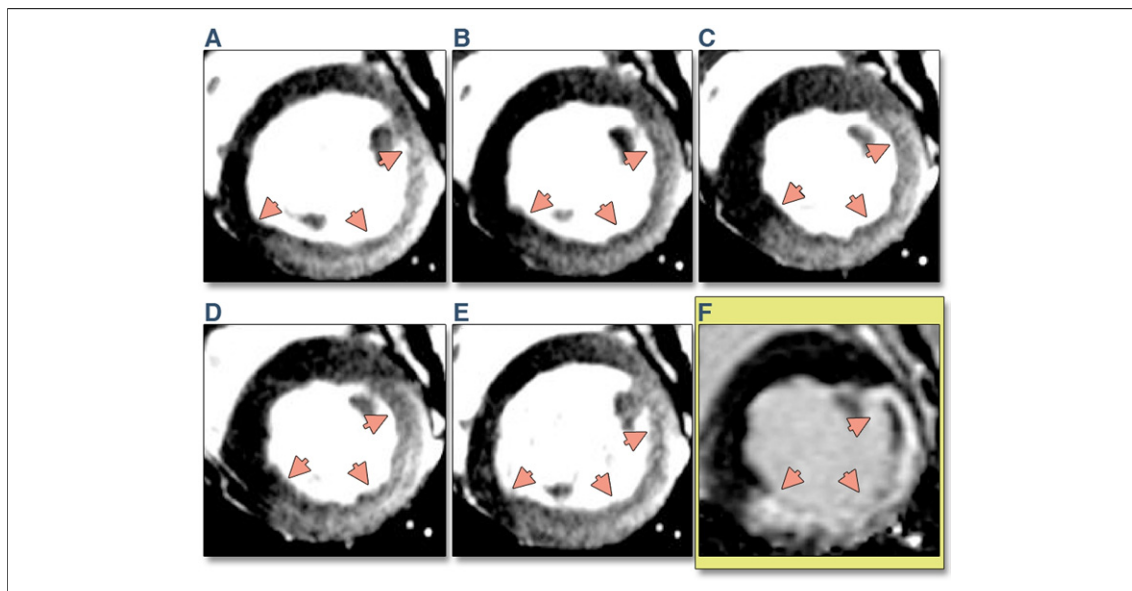


Figure 2. Cardiac Phase-Resolved Edema Images and LGE From Swine

Cine bSSFP-based short-axis magnetic resonance images (A to E) with the corresponding LGE image obtained in late systole (F) in a swine that received a complete occlusion of the left circumflex artery for 90 min followed by reperfusion. The set of cine images, acquired 3 days post-infarction, clearly shows a signal increase in the posterior wall, which is perfused by the left circumflex coronary artery. Also note the close correspondence between regional signal correspondence between bSSFP (A to E) and LGE (F) images. The trigger times for the images: 0 ms (A), 123 ms (B), 245 ms (C), 368 ms (D), 490 ms (E), LGE: 293 ms (F). Arrows indicate the site of infarction. Abbreviations as in Figure 1.

RESULTS

Animal studies. Two of the 15 mini-pigs died of a fatal ventricular arrhythmia. A total of 13 pigs completed the protocol and were available for analysis. Based on LGE-CMR images obtained over the whole left ventricle in each animal, 2 to 4 short-axis slices per pig were observed to have hyperintense myocardial territories consistent with AMI.

A set of typical short-axis cine bSSFP images obtained from the midventricle of a mini-pig and the corresponding LGE-CMR image (at end-systole) are shown in Figure 2. The hyperintense areas, computed on the basis of threshold-based detection performed on bSSFP and LGE images, were highly correlated (Pearson's $R = 0.83$, $p < 0.01$) (Fig. 3), with the line of best fit given by $A_{SSFP} = 1.07A_{LGE} + 0.41$, where A_{SSFP} and A_{LGE} denote the hyperintense myocardial area (cm^2) measured from the bSSFP and LGE images, respectively. The SNR of the infarction zones on bSSFP images was significantly higher than that of the remote myocardium (bSSFP SNR: 85.9 ± 8.4 [infarct] vs. 59.4 ± 7.2 [remote]), resulting in a CNR of 37.2 ± 12.6 . The mean SNR values in healthy (59.4) and affected (85.9) regions with a pooled SD of 15.6 were significantly different ($p < 0.0001$).

Healthy volunteers. In healthy volunteers, the signal measured in the anterior, septal, inferior, and lateral walls of the myocardium was homogeneous (SI ante-

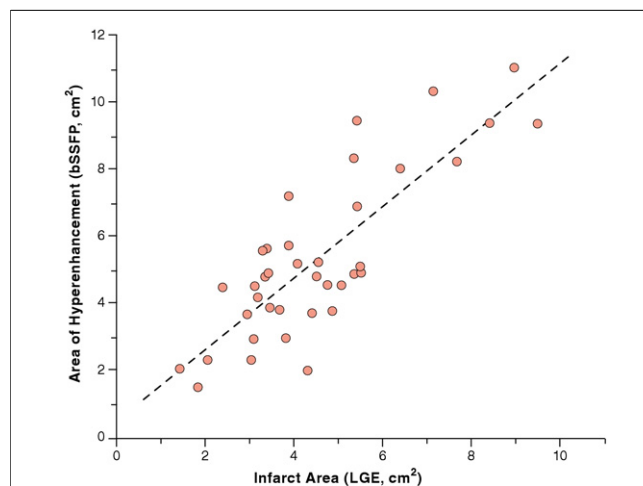


Figure 3. Scatterplot Showing the Correlation Between Infarct Area and Area of Edema Computed From bSSFP

Correlation between infarct area computed from LGE (A_{LGE}) and area of edema computed from bSSFP (A_{SSFP}) images obtained from mini-pigs at late systole is shown. The line of best fit is shown as a dashed line. Equation for line of best fit: $A_{SSFP} = 1.07 A_{LGE} + 0.41$. A strong correlation was observed between the 2 measures of infarct area ($R = 0.83$, $p < 0.001$) with A_{SSFP} being larger than A_{LGE} (slope > 1). Abbreviations as in Figure 1.

rior: 162 ± 12 , SI septum: 165 ± 4 , SI inferior: 160 ± 10 , SI lateral: 151 ± 14 ; analysis of variance $p = 0.08$). **Patients.** From the 27 patients without MVO, 1 patient was excluded because of the absence of CMR findings consistent with AMI, despite a clinical diagnosis of STEMI. The remaining 26 patients (age 57 ± 9 years, 4 women) available for analysis had infarcts in the anterior/septal territory ($n = 13$), inferior territory ($n = 9$), or lateral territory ($n = 4$). Example images from different infarct locations are shown in Figure 4; phase-resolved images from a representative patient are shown in Figure 5. Ten patients with MVO were all male (age 58 ± 9 years) and had MI of the anterior-septal territory ($n = 5$), inferior territory ($n = 4$), or lateral territory ($n = 1$).

On T2-STIR images, the SI in the infarct zone was higher than that in remote myocardium (SI: 373 ± 107 [infarct] vs. 229 ± 75 [remote], $p < 0.001$). Likewise, on the corresponding bSSFP CMR (matched for cardiac phase), the SI in the infarcted myocardium was greater than that of remote myocardium (bSSFP SI: 253 ± 41 [infarct] vs. 162 ± 28 [remote], $p < 0.001$). The infarction-

to-remote myocardium contrast measured on T2-STIR was not different from the contrast measured on bSSFP (contrast T2-STIR: 67 ± 33 vs. bSSFP: 59 ± 26 , $p = 0.31$). Likewise, the normalized CNR was also not different between T2-STIR and bSSFP (CNR_{norm} : 8.08 ± 4.14 [T2-STIR] vs. 7.50 ± 2.96 [bSSFP], $p = 0.53$).

The mean infarction volume (single slice) on LGE-CMR was 4.1 ± 1.4 ml. Edema volumes on T2-STIR images correlated well with edema volumes measured on bSSFP images (Pearson $R = 0.86$, $p < 0.001$) (Fig. 6). The volume of edematous tissue (single slice) measured on T2-STIR correlated with infarct size (Pearson $R = 0.54$, $p < 0.01$); edematous tissue volumes on bSSFP also correlated with infarct size (Pearson $R = 0.47$, $p = 0.02$). The edema volume measured by T2-STIR were not significantly different from those measured with bSSFP (volume of edema on single slice: 6.0 ± 2.3 ml (T2-STIR) vs. 4.9 ± 2.1 ml (bSSFP), $p = 0.07$). A Bland-Altman plot displaying the difference between the measurements using both methods is shown in Figure 7.

Receiver-operator characteristic analysis of bSSFP images obtained from patients and volunteers

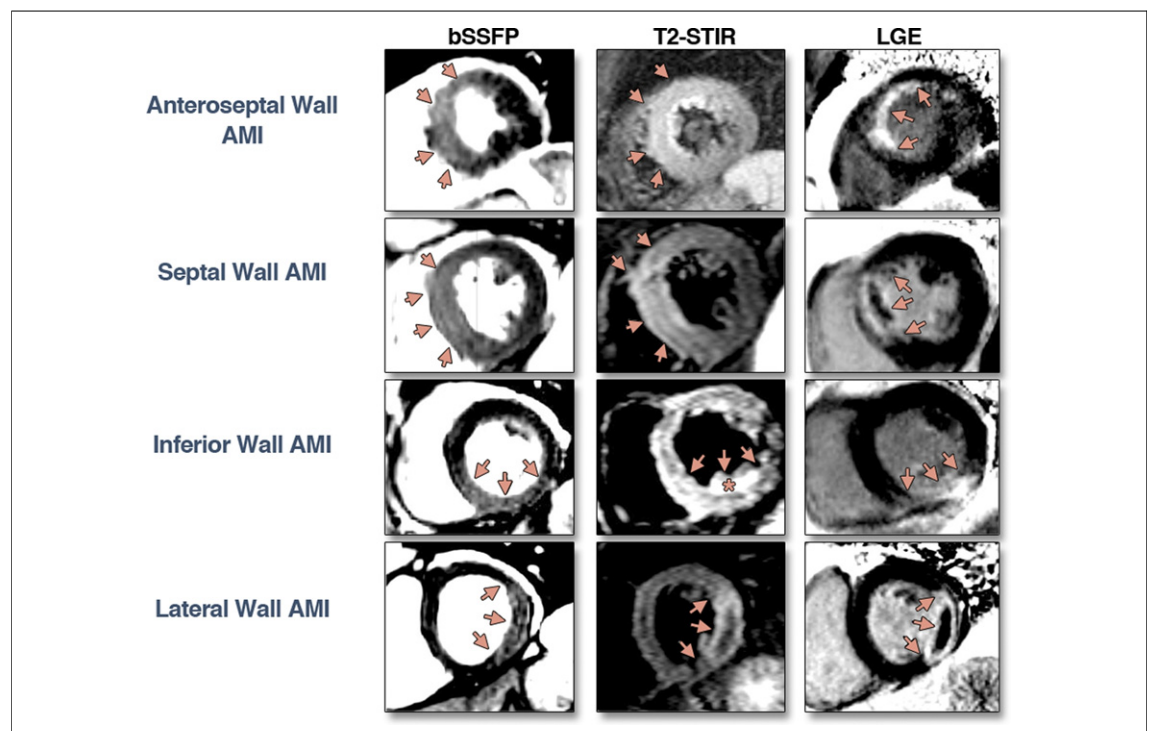


Figure 4. Example Images From Patients With Reperfused STEMI

(First row) Anterior-septal STEMI in a 48-year-old man. (Second row) Septal STEMI in a 63-year-old man. (Third row) Inferior STEMI in a 61-year-old man. (Fourth row) Lateral wall STEMI in a 42-year-old man. The bSSFP area of hyperintense signal (Left column) corresponds well to the region of high signal on T2-STIR (Middle column), but it exceeds the area of irreversible injury as imaged by LGE (Right column). AMI = acute myocardial infarction; other abbreviations as in Figure 1.

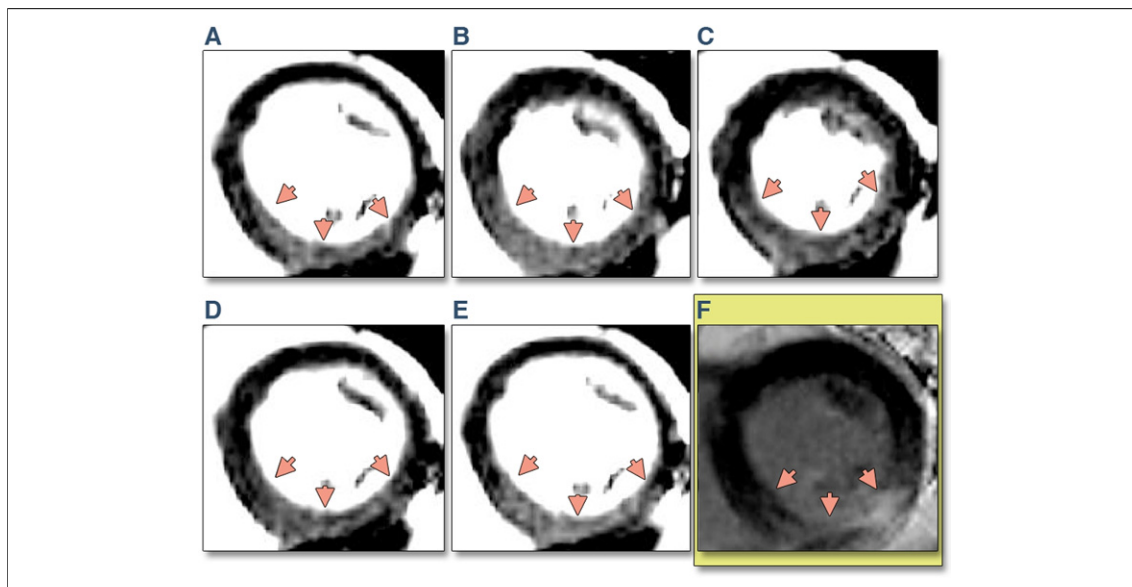


Figure 5. Cardiac Phase-Resolved Edema Images and LGE From a Patient With an Inferior Wall MI

Cine bSSFP-based short-axis cardiac magnetic resonance images (A to E) Cine with the corresponding LGE image obtained in late systole (F) from a patient with acute reperfused STEMI in the territory of the right coronary artery. Note the close correspondence between signal increase patterns between the bSSFP (A to E) and LGE (F) images. The trigger times for the images: 0 ms (A), 198 ms (B), 396 ms (C), 594 ms (D), 792 ms (E), LGE: 455 ms (F). Arrows indicate the site of myocardial infarction (MI). Abbreviations as in Figure 1.

showed the following: 0.99 area under the curve, 96% sensitivity, and 100% specificity.

Zones of MVO consistently yielded reduced SI on bSSFP images compared with the infarction zone without MVO (mean SI from infarcted regions with MVO was 262 ± 27 and MVO zone was 197 ± 33 , $p < 0.001$ for the difference). The contrast between MVO and non-MVO infarction territories was $25 \pm 8\%$. The mean SI from MVO territories was still higher than that from remote myocardium (MVO zone: 197 ± 33 , remote myocardium: 154 ± 41 ; $p < 0.05$ for the difference).

DISCUSSION

We demonstrated that cine bSSFP can detect edema-related signal in reperfused acute myocardial infarcts, in a swine model as well as in patients. In every animal and patient, the bSSFP signal was higher in the acute myocardial infarct zone compared with remote myocardium. Consistent with myocardial edema and the representation of the area at risk (4,12), the zone of high signal on bSSFP was consistently larger than the zone of irreversible injury as assessed by LGE-CMR in animals and patients. The volume of edema measured by bSSFP was not different from that on T2-STIR, on a slice-to-slice basis. Receiver-operator characteristic analysis revealed that T2-STIR and bSSFP images

have nearly the same sensitivity and specificity for identifying myocardial edema associated with STEMI. Zones of MVO yielded a lower signal on bSSFP compared with infarcted tissue without MVO.

T2-weighted imaging plays a key role in the assessment of patients with MI. Its ability to detect myocardial edema (2,8) allows the differentiation of

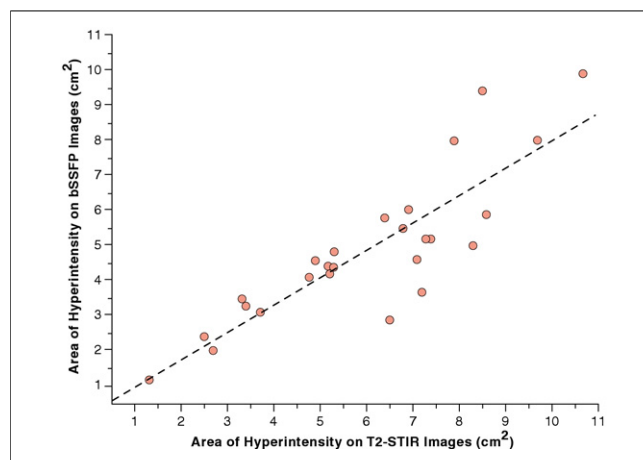


Figure 6. Relation Between the Area of Hyperenhancement on T2-STIR and bSSFP Images

Scatterplot displaying the correlation between edematous areas (in patients) measured from T2-STIR and bSSFP with a semiquantitative analysis. The dotted line indicates the line of best fit. A strong correlation was observed between the 2 measures of edematous areas ($R = 0.86$, $p < 0.001$). Abbreviations as in Figure 1.

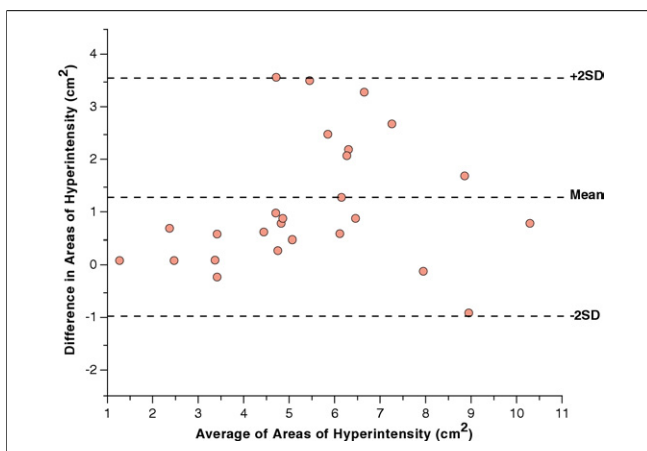


Figure 7. Bland-Altman Analysis of Edema Volume From T2-STIR and bSSFP

There was no statistically significant difference between edema volume on T2-STIR and bSSFP using a paired *t* test (see Results section). Abbreviations as in Figure 1.

acute from chronic myocardial injury (1), the measurement of the area at risk (4,13), and the identification of the perfusion territory subject to ischemic injury. This facilitates the diagnosis of the culprit coronary artery (1). In conjunction with LGE-CMR, T2-weighted CMR allows the assessment of myocardial salvage (12,14). Commonly, T2-weighted fast spin-echo images, limited to a single cardiac phase, are clinically used to assess myocardial edema. The approach that we present here using bSSFP has important advantages over the most commonly used T2-weighted edema imaging methods from a clinical as well as a research perspective.

Clinical perspective. Time is of the essence when using CMR because of the high operating costs of scanners and required staff. Any approach that successfully reduces scanner time will lead to more cost-efficient protocols. Time-efficient imaging protocols benefit patients with acute heart disease such as MI because a delay in therapy in the acute phase is associated with an increase in mortality. Although the benefits of T2-weighted CMR in patients suspected of having a non-ST-segment elevation acute coronary syndrome has been demonstrated (3), the prescription of the complete imaging protocol requires approximately 45 min of scan time, which may not be easily tolerated by the patient. Likewise, in hospitalized patients with acute reperfused STEMI, it is important to keep imaging times as short as possible because these patients are at risk of life-threatening arrhythmia and heart failure. In commonly used CMR protocols, approximately one third of that imaging time is dedicated to whole-heart T2-weighted imaging. De-

veloping equivalent information from bSSFP would provide opportunities to save nearly 15 min of valuable time by obtaining edema and function information (“2 for 1”). This may help to increase patient through-put, decrease waiting time for CMR studies, and make CMR available for more patients.

Research perspective. Although the role of edema in AMI is largely recognized, several questions regarding edema pathophysiology remain unsolved. The imaging approach that we investigated can be applied in a cine manner. This would lay the groundwork for further investigation into the effects of edema on infarction pathophysiology at a moderately high temporal resolution and the investigation of edema at different phases of the cardiac cycle. Edema plays a role in a number of nonischemic cardiomyopathies as well (15–17); future investigations would have to establish the role of bSSFP imaging for edema in these settings.

Study limitations. This was a pilot study with a limited sample size in animals and humans. Nevertheless, the results are consistent across the different analysis groups (animals, healthy volunteers, and patients with AMI). In healthy subjects and patients, to remove potential coil bias, the body coil was used. This may lead to a reduction in the SNR compared with what one would expect with a cardiac (surface) coil. However, by using the body coil, a uniform signal was achieved for all myocardial walls. We deemed a uniform signal with the body coil to be more important than the optimal SNR with a cardiac coil. Nevertheless, even with the body coil applied here, the SNR was sufficient for clinical imaging. Technical improvements that lead to better coil bias corrections are expected to enable the use of the cardiac surface coil for edema imaging with cine bSSFP. This will significantly increase the SNR and the ability to visualize edema without manual windowing in bSSFP images.

Shimming is critically important for the use of myocardial edema imaging with bSSFP; incorrect shims can significantly degrade image quality and assessment of edema. Moreover, because this study used conventional cine bSSFP imaging to identify myocardial edema, possibilities of pulse sequence modifications to optimize the SNR and CNR for edema assessment with cine bSSFP imaging need to be investigated. Given the lack of difference between the CNR_{norm} of T2-STIR and bSSFP approaches, one method to increase the CNR of bSSFP acquisitions is to decrease the acquisition bandwidth. Although this is likely to increase the TR, which may make bSSFP imaging more sensitive to off-

resonance effects, careful shimming and center frequency selection may help overcome these artifacts. Alternatively, image-averaging approaches may be used to increase the CNR of bSSFP-based edema imaging (18).

In this study, bSSFP, T2-STIR, and LGE images were acquired from only a single (midventricular) slice per patient. This prevented us from reporting true volumetric comparison of edema between T2-STIR and bSSFP for each patient.

The receiver-operator characteristic analyses and the sensitivity and specificity measures may be inflated due to the combination of STEMI patients and healthy controls. A more detailed study in a larger population is necessary to more accurately estimate the sensitivity and specificity of bSSFP CMR for detecting myocardial edema in the setting of AMI.

Although the threshold-based semiquantitative image analysis applied here readily detected edema-related hyperintense signals in the affected regions, the performance of a visual nonquantitative image analysis

was not assessed in this study. Manual adjustment of image display for window and contrast may be necessary for optimal visualization of the edema zone.

CONCLUSIONS

This translational study shows that myocardial edema from STEMI can be detected using cine bSSFP imaging, with image contrast similar to T2-STIR. This new imaging approach allows evaluation of cardiac function and edema simultaneously, thereby reducing patient scan time and increasing efficiency. Further work is necessary to optimize edema contrast in bSSFP images.

Reprint requests and correspondence: Dr. Rohan Dharmakumar, Biomedical Imaging Research Institute, Department of Biomedical Sciences, Cedars-Sinai Medical Center, 8700 Beverly Boulevard, Suite G-149D, Los Angeles, California 90048. *E-mail:* robandkumar@csmc.edu.

REFERENCES

1. Abdel-Aty H, Zagrosek A, Schulz-Menger J, et al. Delayed enhancement and T2-weighted cardiovascular magnetic resonance imaging differentiate acute from chronic myocardial infarction. *Circulation* 2004;109:2411-6.
2. Abdel-Aty H, Cocker M, Meek C, Tyberg JV, Friedrich MG. Edema as a very early marker for acute myocardial ischemia: a cardiovascular magnetic resonance study. *J Am Coll Cardiol* 2009;53:1194-201.
3. Cury RC, Shash K, Nagurney JT, et al. Cardiac magnetic resonance with T2-weighted imaging improves detection of patients with acute coronary syndrome in the emergency department. *Circulation* 2008;118:837-44.
4. Aletras AH, Tilak GS, Natanzon A, et al. Retrospective determination of the area at risk for reperfused acute myocardial infarction with T2-weighted cardiac magnetic resonance imaging: histopathological and displacement encoding with stimulated echoes (DENSE) functional validations. *Circulation* 2006;113:1865-70.
5. Kellman P, Aletras AH, Mancini C, McVeigh ER, Arai AE. T2-prepared SSFP improves diagnostic confidence in edema imaging in acute myocardial infarction compared to turbo spin echo. *Magn Reson Med* 2007;57:891-7.
6. Haacke EM, Brown RW, Thompson MR, Venkatesan R. *Magnetic Resonance Imaging: Physical Principles and Sequence Design*. New York: John Wiley & Sons Inc., 1999:451-512.
7. Bieri O, Scheffler K. On the origin of apparent low tissue signals in balanced SSFP. *Magn Reson Med* 2006;56:1067-74.
8. Higgins CB, Herfkens R, Lipton MJ, et al. Nuclear magnetic resonance imaging of acute myocardial infarction in dogs: alterations in magnetic relaxation times. *Am J Cardiol* 1983;52:184-8.
9. Haraldseth O, Jones RA, Schjøtt J, Rinck PA, Jynge P, Oksendal AN. Early detection of regional myocardial ischemia in ex vivo piglet hearts: MR imaging with magnetization transfer. *J Magn Reson Imaging* 1994;4:603-8.
10. Weber OM, Speier P, Scheffler K, Bieri O. Assessment of magnetization transfer effects in myocardial tissue using balanced steady-state free precession (bSSFP) cine MRI. *Magn Reson Med* 2009;62:699-705.
11. Bondarenko O, Beek AM, Hofman MB, et al. Standardizing the definition of hyperenhancement in the quantitative assessment of infarct size and myocardial viability using delayed contrast-enhanced CMR. *J Cardiovasc Magn Reson* 2005;7:481-5.
12. Friedrich MG, Abdel-Aty H, Taylor A, Schulz-Menger J, Messroghli D, Dietz R. The salvaged area at risk in reperfused acute myocardial infarction as visualized by cardiovascular magnetic resonance. *J Am Coll Cardiol* 2008;51:1581-7.
13. Garcia-Dorado D, Oliveras J, Gili J, et al. Analysis of myocardial oedema by magnetic resonance imaging early after coronary artery occlusion with or without reperfusion. *Cardiovasc Res* 1993;27:1462-9.
14. Ibanez B, Prat-Gonzalez S, Speidl WS, et al. Early metoprolol administration before coronary reperfusion results in increased myocardial salvage: analysis of ischemic myocardium at risk using cardiac magnetic resonance. *Circulation* 2007;115:2909-16.
15. Friedrich MG, Sechtem U, Schulz-Menger J, et al. Cardiovascular magnetic resonance in myocarditis: a JACC white paper. *J Am Coll Cardiol* 2009;53:1475-87.
16. Abdel-Aty H, Cocker M, Friedrich MG. Myocardial edema is a feature of Tako-Tsubo cardiomyopathy and is related to the severity of systolic dysfunction: insights from T2-weighted cardiovascular magnetic resonance. *Int J Cardiol* 2009;132:291-3.
17. Melacini P, Corbetti F, Calore C, et al. Cardiovascular magnetic resonance signs of ischemia in hypertrophic cardiomyopathy. *Int J Cardiol* 2008;128:364-73.
18. Kellman P, Larson AC, Hsu LY, et al. Motion-corrected free-breathing delayed enhancement imaging of myocardial infarction. *Magn Reson Med* 2005;53:194-200.

Key Words: cardiac magnetic resonance ■ cardiac phase-resolved ■ edema ■ infarction ■ ST-segment elevation myocardial infarction.